Experimental and Analytical Reexamination of Classic Concrete Beam Tests

F. J. Vecchio[1] and W. Shim[2]

Abstract: The classic series of beam tests conducted by Bresler and Scordelis some 40 years ago to investigate the behavior of reinforced concrete in shear, is commonly regarded as a benchmark against which finite element analysis models can be calibrated. A nominally identical set of beams was recently tested at the University of Toronto. Aspects of behavior of the original and duplicate beams are compared and discussed, including load–deformation response, load capacity, and failure mode. Generally, it was found that most aspects of behavior were well replicated. Test observations reveal that the behavior of the beams is highly influenced by crushing of concrete beneath and adjacent to the loading plates. In the case of the beams containing no shear reinforcement, failure was influenced by the reinforcement anchorage plates. The disturbances around the loading plates and anchor plates introduce complex three-dimensional effects, making the modeling of these beams using two-dimensional finite element techniques difficult. However, accuracy is substantially improved if out-of-plane confinement effects are considered. In addition to some insights on the behavior of the original beams, and on factors that should be considered in their finite element modeling, the duplicate tests also provide information on postpeak behavior.

DOI: 10.1061/(ASCE)0733-9445(2004)130:3(460)

CE Database subject headings: Beams; Concrete; Tests; Ductility; Finite elements; Models; Shear.

Introduction

In the still-evolving field of nonlinear finite element analysis of reinforced concrete structures, the pioneering work started by Scordelis in the early 1960s was instrumental in defining the concepts and approaches generally followed by the research community since. His defining contributions in this area were recently recognized by a dedicated volume on the state of the art (Willam and Tanabe 2001), containing works from many current leading researchers.

Among Professor Scordelis' many contributions was a seminal paper describing the testing of a series of 12 reinforced concrete beams (Bresler and Scordelis 1963), aimed primarily at investigating shear-critical behavior, but also at providing data to support finite element development work. The beams tested covered a wide range of reinforcement and span conditions, and hence, a range of influencing factors and failure modes. These beams soon came to be regarded as a classic test series. They have since been used extensively as benchmark data for calibrating or verifying finite element models for reinforced concrete (e.g., ASCE 1982), particularly for modeling of beams critical in shear.

The use of the Bresler–Scordelis beams as a benchmark series is due, in part, to the high quality and thorough documentation of the tests. Also contributing to their frequent use is the fact that the tests represent a difficult challenge in modeling, with many finite element formulations failing to provide accurate simulations of the behavior exhibited by these beams.

A test program was recently undertaken at the University of Toronto to recreate, as much as possible, the Bresler–Scordelis test series. There were several objectives in doing so. First, it was sought to determine the extent of repeatability of the test results, particularly with respect to load capacity and failure mode, given that there would be some unavoidable differences in construction and testing procedures. Information on postpeak response was also sought; the load–deflection response reported for the Bresler–Scordelis beams abruptly terminated at the peak loads. Additional insight into the behavior of the beams, such as the nature of important influencing factors and critical behavior mechanisms, would also hopefully emerge from new first-hand test observations. Finally, insight into critical factors in the accurate finite element modeling of these beams was sought.

Details of Bresler–Scordelis Beams

The 12 beams tested by Bresler and Scordelis (1963) consisted of four series of three beams; each series differed in amount of longitudinal reinforcement, amount of shear reinforcement, span length, cross-section dimensions, and concrete strength. All beams were of rectangular cross section with the same overall depth of 552 mm. Cross-section details are given in Fig. 1; additional details are given in Table 1. (To facilitate comparisons, the specimen names of the Bresler–Scordelis beams will be prefixed with BS.) All bottom longitudinal reinforcement was provided by No. 9 bars, while No. 4 bars were used for all top longitudinal reinforcement. Shear reinforcement, where provided, was in the form of closed stirrups constructed from No. 2 bars. To prevent bond failure due to possibly insufficient anchorage, the bottom longitudinal reinforcement was extended through the ends of the beam and anchored to 35 mm steel end plates via special anchor

[1]Professor, Dept. of Civil Engineering, Univ. of Toronto, Toronto, Canada. E-mail: fjv@civ.utoronto.ca

[2]Graduate Student, Dept. of Civil Engineering, Univ. of Toronto, Toronto, Canada.

Note. Associate Editor: Joseph M. Bracci. Discussion open until August 1, 2004. Separate discussions must be submitted for individual papers. To extend the closing date by one month, a written request must be filed with the ASCE Managing Editor. The manuscript for this paper was submitted for review and possible publication on June 27, 2002; approved on March 24, 2003. This paper is part of the ***Journal of Structural Engineering***, Vol. 130, No. 3, March 1, 2004. ©ASCE, ISSN 0733-9445/2004/3-460–469/$18.00.

J. Struct. Eng. 2004.130:460-469.

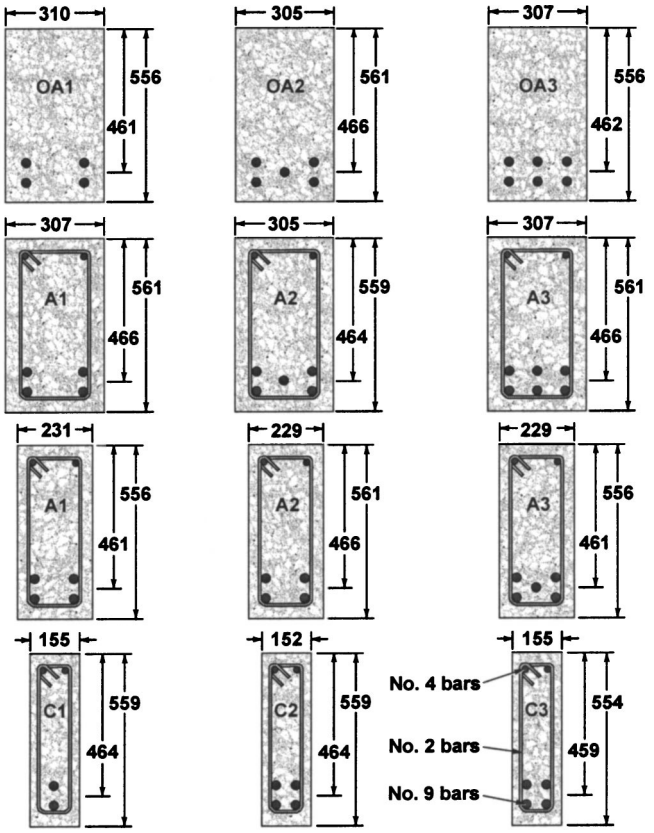

Fig. 1. Cross-section details of Bresler–Scordelis beams

nuts. Note that the OA series of beams contained no shear reinforcement. Also note that heavy amounts of flexural reinforcement were used in attempting to make the beams shear critical. Material properties, with respect to the concrete, longitudinal reinforcement, and shear reinforcement are summarized in Table 2. The maximum aggregate size was 20 mm ($\frac{3}{4}$ in.).

The test setup used to perform the experiments is schematically shown in Fig. 2. All beams were subjected to monotonic center-point loading, with a force-controlled loading procedure employed. The test beams were typically first loaded to about 30% of ultimate in two or three increments, and then unloaded. Load was reapplied in 40 kN increments per load stage, to a point near ultimate, and then in 20 kN increments until failure occurred.

It should be noted that the Bresler–Scordelis beams were all tested at a fairly young age, likely with the concrete still moist. The procedure followed had the beams stripped from their formwork at four days after casting, and moist cured for seven days thereafter using wet burlap. All beams were tested at 13 days of age.

Details of Toronto Beams

The 12 Toronto beams were nominally identical to the Bresler–Scordelis beams in terms of cross-section dimensions and amount of reinforcement provided. Cross-section details are given in Fig. 3, and the beam profiles are shown in Fig. 4. Table 3 provides additional relevant details. (To facilitate comparisons, the specimen names given to the Toronto beams are the same as those for the corresponding Bresler–Scordelis beams except prefixed with VS.) Due to unavailability of adequate amounts of the imperial-sized bars, metric-sized bars were used instead. M25 and M30 bars ($A_s = 500$ and 700 mm^2, respectively) were used in various combinations to obtain roughly the same reinforcement ratios as with the Bresler–Scordelis beams. Similarly, M10 bars ($A_s = 100$ mm^2) were used for the compression reinforcement, and D4 and D5 deformed bar ($A_s = 25.7$ and 32.2 mm^2, respectively) were used for the stirrups. As with the original beams, the bottom longitudinal bars were extended past the ends of the beam and anchored to a 25-mm-thick end plate, in this case, by welding. Material properties of the concrete (at time of beam test), longitudinal reinforcement, and shear reinforcement for the Toronto beams are summarized in Table 4. The maximum aggregate size was 20 mm ($\frac{3}{4}$ in.).

The test setup used to perform the Toronto experiments is schematically shown in Fig. 5. Note that a servocontrolled MTS 2700 kN universal testing machine was used to apply center-point loading. As with the Bresler–Scordelis beams, the loads were initially applied in 40 kN increments per load stage. Near ultimate, loading was switched to displacement control, allowing the continuation of the tests into the postpeak load regimes. The specimens were instrumented for electronic monitoring of midspan and end deflections, and for strains in the longitudinal reinforcement in the midspan regions. Note that the Toronto beams

Table 1. Cross-Section Details of Bresler–Scordelis Beams

Beam number	b (mm)	h (mm)	d (mm)	L (mm)	Span (mm)	Bottom steel	Top steel	Stirrups
OA1	310	556	461	4,100	3,660	4 No. 9	—	—
OA2	305	561	466	5,010	4,570	5 No. 9	—	—
OA3	307	556	462	6,840	6,400	6 No. 9	—	—
A1	307	561	466	4,100	3,660	4 No. 9	2 No. 4	No. 2 at 210
A2	305	559	464	5,010	4,570	5 No. 9	2 No. 4	No. 2 at 210
A3	307	561	466	6,840	6,400	6 No. 9	2 No. 4	No. 2 at 210
B1	231	556	461	4,100	3,660	4 No. 9	2 No. 4	No. 2 at 190
B2	229	561	466	5,010	4,570	4 No. 9	2 No. 4	No. 2 at 190
B3	229	556	461	6,840	6,400	5 No. 9	2 No. 4	No. 2 at 190
C1	155	559	464	4,100	3,660	2 No. 9	2 No. 4	No. 2 at 210
C2	152	559	464	5,010	4,570	4 No. 9	2 No. 4	No. 2 at 210
C3	155	554	459	6,840	6,400	4 No. 9	2 No. 4	No. 2 at 210

J. Struct. Eng. 2004.130:460-469.

Table 2. Material Properties of Bresler–Scordelis Beams

Bar size	Reinforcement: Diameter (mm)	Area (mm^2)	f_y (MPa)	f_u (MPa)	E_s. (MPa)
No. 2	6.4	32.2	325	430	190,000
No. 4	12.7	127	345	542	201,000
No. 9	28.7	645	555	933	218,000

Beam number	Concrete: f'_c (MPa)	f_r (MPa)
OA1	22.6	3.97
OA2	23.7	4.34
OA3	37.6	4.14
A1	24.1	3.86
A2	24.3	3.73
A3	35.1	4.34
B1	24.8	3.99
B2	23.2	3.76
B3	38.8	4.22
C1	29.6	4.22
C2	23.8	3.93
C3	35.1	3.86

were not initially preloaded and unloaded, as was done with the Bresler–Scordelis beams. Also note that the average age at testing was considerably longer; approximately 38 days for the 4.1 m beams, 51 days for the 5.0 m beams, and 127 days for the 6.8 m beams.

While attempts were made to match the Bresler–Scordelis beams as much as possible in terms of dimensions, reinforcement details, and material strengths, some unavoidable variations arose. Table 5 compares the differences in reinforcement amounts; generally, the reinforcement ratios are well matched in most cases. With respect to the shear reinforcement, although the amounts of reinforcement are identical, the yield strengths of the stirrup steel are considerably different and will have some influence on the results. (Differences in the yield strength of the longitudinal reinforcement are largely irrelevant since yielding of the longitudinal steel was not a major factor in most tests.) Note, too, that there are some appreciable differences in concrete strengths between corresponding BS and VS beams, despite best efforts to match them.

Test Observations

The Bresler–Scordelis beams were characterized by three different modes of failure: diagonal–tension ($D-T$), shear–compression ($V-C$), and flexure–compression ($F-C$). The diagonal–tension failures were observed in all beams containing no shear reinforcement. The shear–compression mode was dominant in the intermediate-span beams containing web reinforcement, and the flexure–compression mode prevailed in the long-span beams containing web reinforcement. The failure mode corresponding to each of the 12 Bresler–Scordelis beams, to-

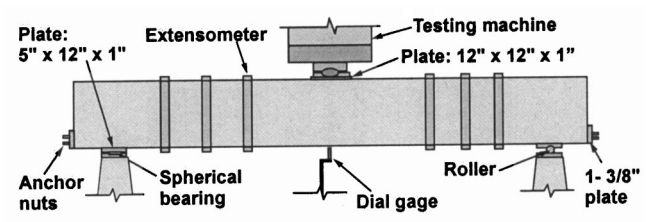

Fig. 2. Test setup for Bresler–Scordelis beams

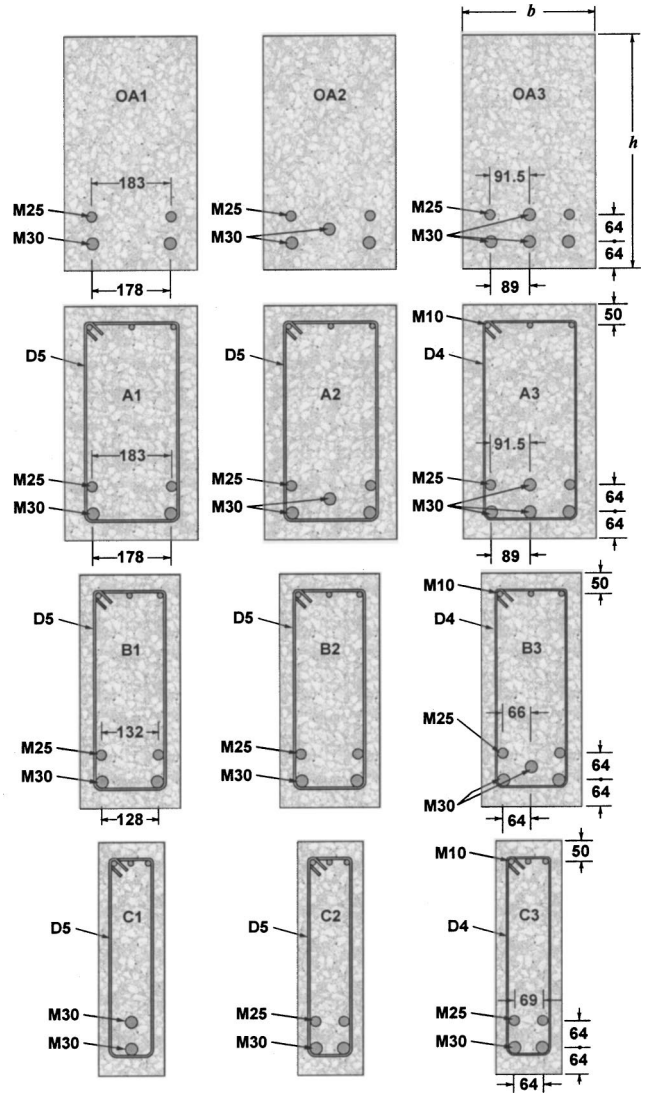

Fig. 3. Cross-section details of Toronto beams

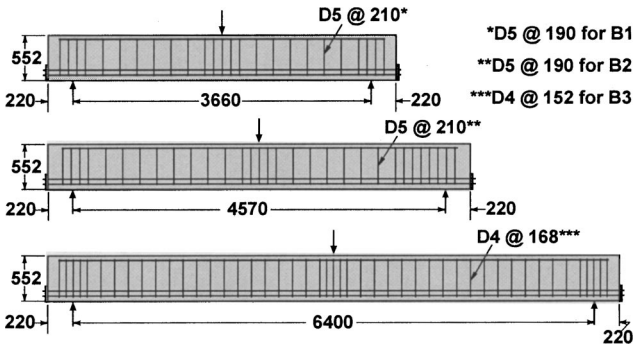

Fig. 4. Elevation details of Toronto beams

J. Struct. Eng. 2004.130:460-469.

Table 3. Cross-Section Details of Toronto Beams

Beam number	b (mm)	h (mm)	d (mm)	L (mm)	Span (mm)	Bottom steel	Top steel	Stirrups
OA1	305	552	457	4,100	3,660	2 M30, 2 M25	—	—
OA2	305	552	457	5,010	4,570	3 M30, 2 M25	—	—
OA3	305	552	457	6,840	6,400	4 M30, 2 M25	—	—
A1	305	552	457	4,100	3,660	2 M30, 2 M25	3 M10	D5 at 210
A2	305	552	457	5,010	4,570	3 M30, 2 M25	3 M10	D5 at 210
A3	305	552	457	6,840	6,400	4 M30, 2 M25	3 M10	D4 at 168
B1	229	552	457	4,100	3,660	2 M30, 2 M25	3 M10	D5 at 190
B2	229	552	457	5,010	4,570	2 M30, 2 M25	3 M10	D5 at 190
B3	229	552	457	6,840	6,400	3 M30, 2 M25	3 M10	D4 at 152
C1	152	552	457	4,100	3,660	2 M30	3 M10	D5 at 210
C2	152	552	457	5,010	4,570	2 M30, 2 M25	3 M10	D5 at 210
C3	152	552	457	6,840	6,400	2 M30, 2 M25	3 M10	D4 at 168

gether with ultimate load capacity and midspan deflection at ultimate load, are given in Table 6. Load–deflection response plots are given in Fig. 6.

A summary of the test observations reported by Bresler and Scordelis is as follows. In the beams controlled by diagonal tension, failure occurred shortly after the formation of the ''critical'' diagonal–tension crack. It was accompanied by longitudinal splitting in the compression zone near the load point, and by horizontal splitting along the tension reinforcement toward the ends of the beam. The critical diagonal cracks formed at approximately 80% of the ultimate load, and deterioration was rapid thereafter. Failure was sudden and brittle-like. In the beams controlled by the shear–compression mode, failure occurred by splitting in the compression zone but without splitting along the tension reinforcement. Diagonal–tension cracks formed at approximately 60% of the ultimate load, and propagated with increased loading but did not indicate visible signs of distress. In the long-span beams controlled by flexure compression, being over-reinforced for flexure, failure occurred by crushing of the concrete in the compression zone near the midspan. Initial flexural cracks formed at loads of approximately 15% of ultimate, and these propagated as loading increased; however, major diagonal–tension cracks did not develop. Failure was, again, sudden and brittle.

The Toronto beams exhibited very similar response, in most respects, to the corresponding Bresler–Scordelis beams. The failure modes, ultimate load capacities, midspan deflections at ultimate load, maximum crack widths, and maximum measured strains in the tension reinforcement are given in Table 6. Load–deflection response plots are given in Fig. 6. Photographs of each test beam, at ultimate load condition, are given in Fig. 7.

In the Toronto beams containing no shear reinforcement (i.e., OA1, OA2, and OA3), behavior was characterized by sudden failure resulting from diagonal–tension cracking. Shortly after its formation, the critical diagonal crack propagated rapidly down to the depth of the top-most layer of tension reinforcement, and then continued as a large horizontal crack to the end of the beam [e.g., see Fig. 8(a)]. Failure was sudden and brittle, with no ductility in the load–deformation response beyond the peak load.

In the beams of intermediate length and containing web reinforcement (ie., A1, A2, B1, B2, C1, and C2), behavior could be characterized as shear flexural in nature. These beams exhibited severe diagonal–tension cracks during later load stages, as shown

Table 4. Material Properties of Toronto Beams

	Reinforcement				
Bar size	Diameter (mm)	Area (mm^2)	f_y (MPa)	f_u (MPa)	E_s (MPa)
M10	11.3	100	315	460	200,000
M25[a]	25.2	500	440	615	210,000
M25[b]	25.2	500	445	680	220,000
M30	29.9	700	436	700	200,000
D4	3.7	25.7	600	651	200,000
D5	6.4	32.2	600	649	200,000

	Concrete			
Beam number	f'_c (MPa)	ε_0 (mm/mm)	E_c (MPa)	f_{sp} (MPa)
OA1	22.6	0.0016	36,500	2.37
OA2	25.9	0.0021	32,900	3.37
OA3	43.5	0.0019	34,300	3.13
A1	22.6	0.0016	36,500	2.37
A2	25.9	0.0021	32,900	3.37
A3	43.5	0.0019	34,300	3.13
B1	22.6	0.0016	36,500	2.37
B2	25.9	0.0021	32,900	3.37
B3	43.5	0.0019	34,300	3.13
C1	22.6	0.0016	36,500	2.37
C2	25.9	0.0021	32,900	3.37
C3	43.5	0.0019	34,300	3.13

[a]Series 2.

[b]Series 1 and 3.

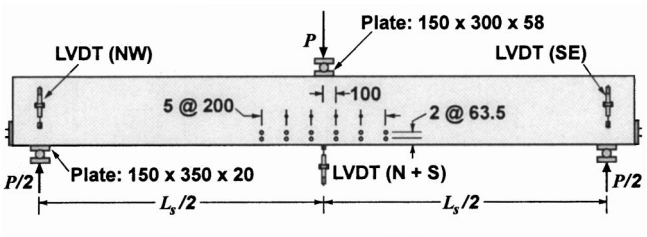

Fig. 5. Test setup for Toronto beams

J. Struct. Eng. 2004.130:460-469.

Table 5. Comparison of Beam Details: (a) Reinforcement Amounts and (b) Concrete Strengths

Beam number	Concrete			Transverse reinforcement			Tension reinforcement			Compression reinforcement		
	$f'_{c\text{-BS}}$ (MPa)	$f'_{c\text{-VS}}$ (MPa)	$f'_{c\text{-BS}}/f'_{c\text{-VS}}$	$\rho_{v\text{-BS}}$ (%)	$\rho_{v\text{-VS}}$ (%)	$\rho_{v\text{-BS}}/\rho_{v\text{-VS}}$	$A_{s\text{-BS}}$ (mm^2)	$A_{s\text{-VS}}$ (mm^2)	$A_{s\text{-BS}}/A_{s\text{-VS}}$	$A'_{s\text{-BS}}$ (mm^2)	$A'_{s\text{-VS}}$ (mm^2)	$A'_{s\text{-BS}}/A'_{s\text{-VS}}$
OA1	22.6	22.6	1.00	—	—	—	2,579	2,400	1.07	253	300	0.84
OA2	23.7	25.9	0.92	—	—	—	3,224	3,100	1.04	253	300	0.84
OA3	37.6	43.5	0.86	—	—	—	3,868	3,800	1.02	253	300	0.84
A1	24.1	22.6	1.07	0.100	0.100	1.00	2,579	2,400	1.07	253	300	0.84
A2	24.3	25.9	0.94	0.100	0.100	1.00	3,224	3,100	1.04	253	300	0.84
A3	35.1	43.5	0.81	0.100	0.100	1.00	3,868	3,800	1.02	253	300	0.84
B1	24.8	22.6	1.10	0.148	0.148	1.00	2,579	2,400	1.07	253	300	0.84
B2	23.2	25.9	0.90	0.148	0.148	1.00	2,579	2,400	1.07	253	300	0.84
B3	38.8	43.5	0.89	0.148	0.147	1.00	3,224	3,100	1.04	253	300	0.84
C1	29.6	22.6	1.31	0.202	0.202	1.00	1,289	1,400	0.92	253	300	0.84
C2	23.8	25.9	0.92	0.202	0.202	1.00	2,579	2,400	1.07	253	300	0.84
C3	35.1	43.5	0.81	0.202	0.201	1.00	2,579	2,400	1.07	253	300	0.84
Mean			0.96			1.00			1.04			0.84

in Fig. 8(b) for beam VS-A1, for example, with crack widths as large as 2.0 mm. However, both the initial distress and final failure occurred by crushing of concrete in the compression zone; there was no accompanying splitting along the tension reinforcement. Flexure cracks in the midspan regions were relatively insignificant, with crack widths generally in the range of 0.5–1.0 mm. Most notable was the crushing of concrete beneath and adjacent to the loading plate, occurring before any shear distress was evident. These beams generally exhibited a small measure of ductility at the peak–load level before a sudden drop off in load capacity occurred.

The long-span beams (i.e., A3, B3, and C3), generally exhibited a flexure–compression failure. Again, failure was induced by crushing of the concrete in the compression zone, notably appearing first under the loading plate. Unlike the intermediate-length beams, diagonal tension cracking was minor if present at all. The flexural crack widths were, in some cases, as high as 1.5 mm. Pronounced yielding of the tension reinforcement was not detected in any beam, although it appeared imminent in some (e.g. beams A3 and B3). The load–deformation response of these beams demonstrated a fair measure of postpeak ductility.

Comparison of Test Results

All 12 Toronto beams experienced a failure nominally similar to the one observed in the corresponding Bresler–Scordelis beam (see Table 6), when classified according to the three modes of failure previously defined. However, in comparing the load–deformation responses for each pair of specimens (Fig. 6), the Toronto beams generally exhibited lower stiffness in the ascending response, and greater deformation at ultimate. This was observed despite deformation control at each load step, which would have minimized short-term creep effects, and despite the some-

Table 6. Test Results for Bresler–Scordelis and Toronto Beams

Beam number	Bresler–Scordelis beams			Toronto beams							
	$P_{u\text{-BS}}$ (kN)	$\delta_{u\text{-BS}}$ (mm)	Failure mode	$P_{u\text{-VS}}$ (kN)	$\delta_{u\text{-VS}}$ (mm)	Failure mode	$w_{s\text{-max}}$ (mm)	$w_{f\text{-max}}$ (mm)	$\epsilon_{s\text{-max}}$ ($\times 10^{-3}$)	$P_{u\text{-BS}}/P_{u\text{-VS}}$	$\delta_{u\text{-BS}}/\delta_{u\text{-VS}}$
OA1	334	6.6	*D–T*	331	9.1	*D–T*	0.25	0.40	0.438	1.01	0.73
OA2	356	11.7	*D–T*	320	13.2	*D–T*	0.30	0.30	0.548	1.11	0.89
OA3	378	27.9	*D–T*	385	32.4	*D–T*	0.25	0.35	0.622	0.98	0.86
A1	467	14.2	*V–C*	459	18.8	*V–C*	2.00	0.50	1.172	1.02	0.76
A2	489	22.9	*V–C*	439	29.1	*V–C*	0.90	1.40	1.635	1.12	0.79
A3	467	35.8	*F–C*	420	51.0	*F–C*	0.25	1.60	2.827	1.11	0.70
B1	445	13.7	*V–C*	434	22.0	*V–C*	0.90	0.75	2.535	1.03	0.62
B2	400	20.8	*V–C*	365	31.6	*V–C*	0.50	1.60	2.867	1.10	0.66
B3	356	35.3	*F–C*	342	59.6	*F–C*	0.30	1.60	2.708	1.04	0.59
C1	311	17.8	*V–C*	282	21.0	*V–C*	0.60	2.50	2.809	1.11	0.85
C2	325	20.1	*V–C*	290	25.7	*V–C*	0.50	0.40	0.726	1.12	0.78
C3	269	36.8	*F–C*	265	44.3	*F–C*	0.25	0.90	1.757	1.02	0.83
									Mean	1.06	0.75
									COV(%)	5.12	9.61

J. Struct. Eng. 2004.130:460-469.

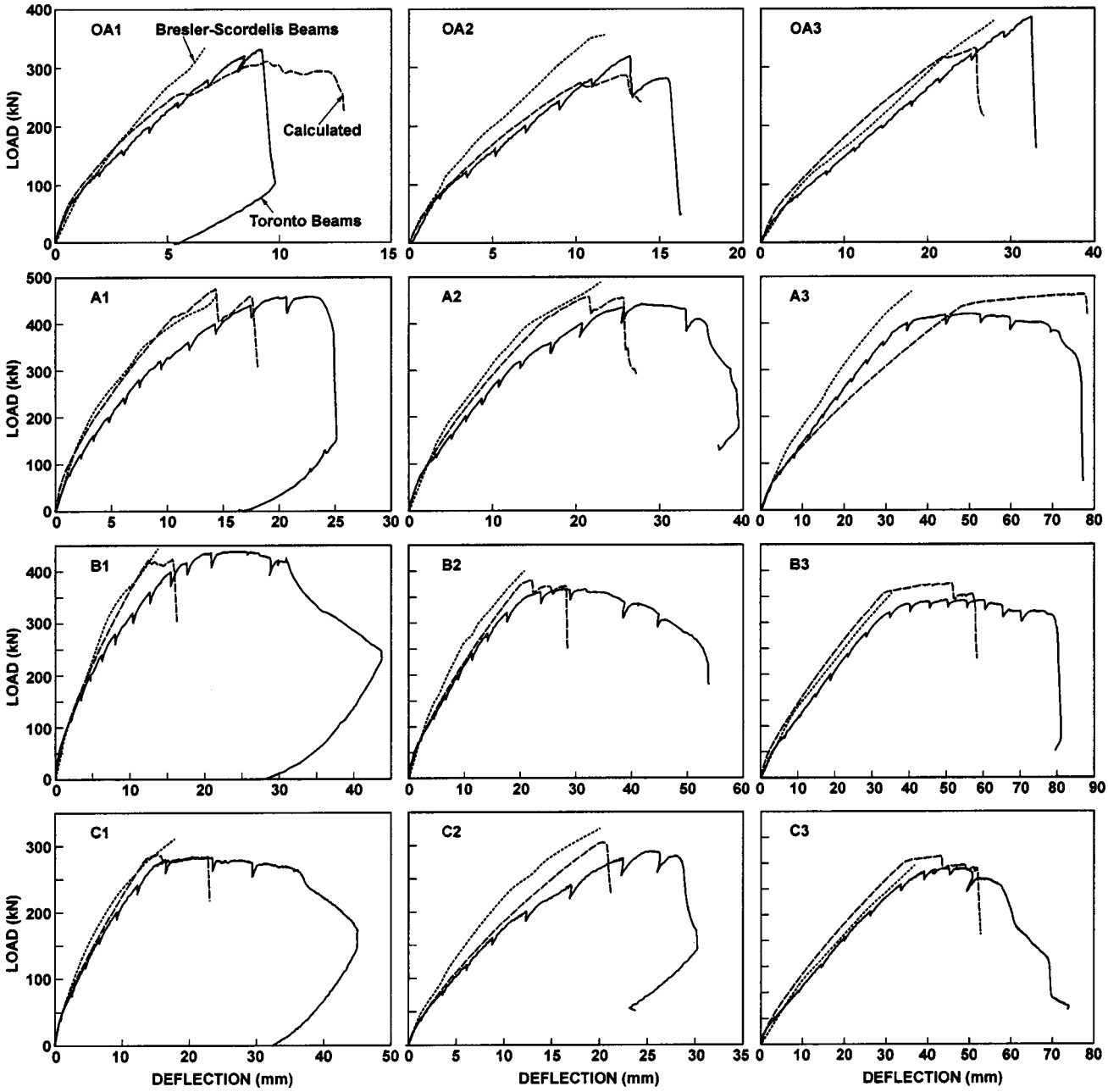

Fig. 6. Load–deflection responses

what higher concrete strengths in the Toronto beams. The Bresler–Scordelis beams did contain approximately 4% more flexural tension reinforcement, on average, explaining to some extent the greater stiffnesses. Also, preloading of the Bresler–Scordelis beams may have had some influence.

Compared in Table 6 are the ultimate load capacities of the two set of beams. The Toronto beams consistently attained slightly lower ultimate loads than did the corresponding Bresler–Scordelis beams. The ratio of the peak load of the Bresler–Scordelis beams to that of the Toronto beams (i.e., $P_{u,\text{exp-BS}}/P_{u,\text{exp-VS}}$) had a mean of 1.06 and a coefficient of variation of 5.1%. With the percentages of longitudinal and transverse reinforcement reasonably similar, and with the concrete strength slightly higher and the yield strength of the transverse reinforcement significantly higher in the Toronto beams, one might have expected slightly higher strengths with the Toronto beams.

The Toronto beams generally achieved greater deflections at peak load than did the Bresler–Scordelis beams (see Table 6). The ratio of the deflection of the Bresler–Scordelis beams to that of the Toronto beams (i.e., $\delta_{u,\text{exp-BS}}/\delta_{u,\text{exp-VS}}$) had a mean of 0.75 and a coefficient of variation of 9.6%. The relatively flat ultimate load plateau observed in some of the Toronto beams may amount to some of the dissimilarity in results. This, in turn, may be a result of the higher yield stress of the transverse reinforcement providing more ductility to the response.

Finite Element Analysis

Two-dimensional nonlinear finite element analyses were undertaken for each of the two sets of test beams. The analysis were performed using program VecTor2, developed at the University of

J. Struct. Eng. 2004.130:460-469.

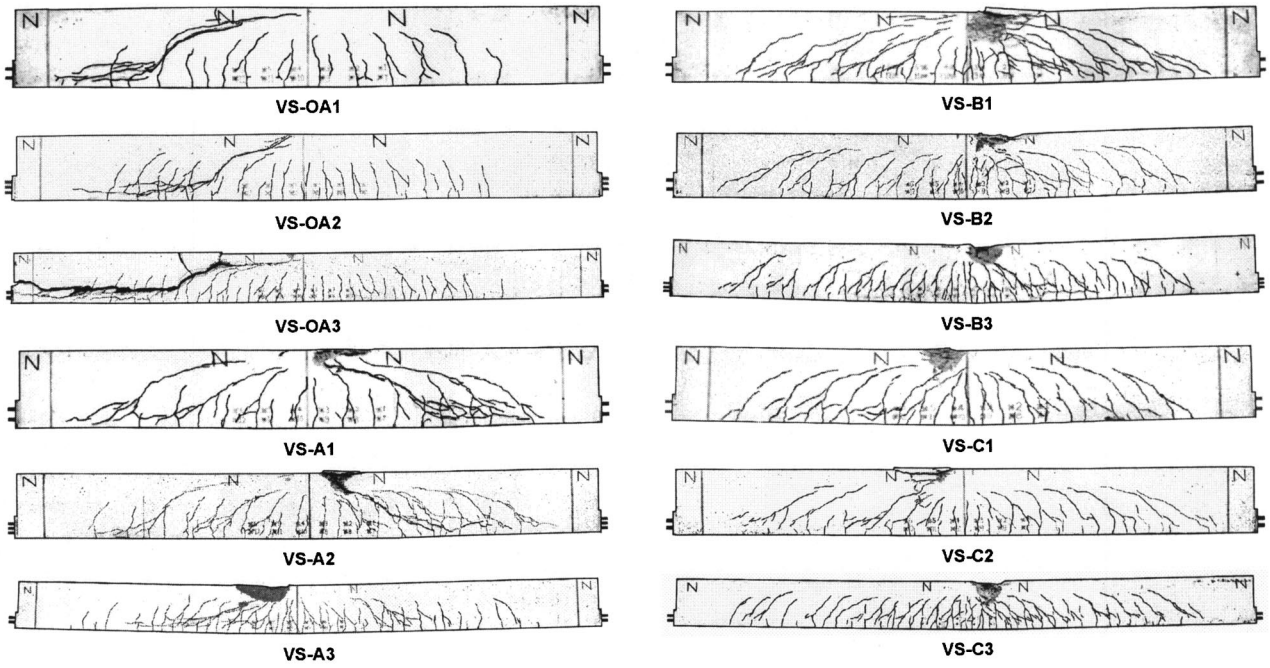

Fig. 7. Toronto test beams at ultimate load

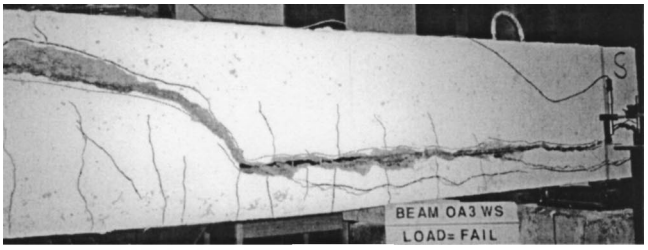

(a) VS-OA3

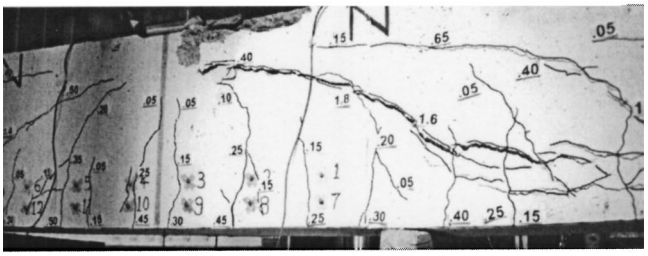

(b) VS-A1

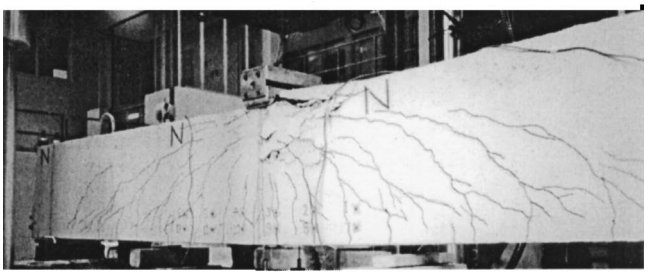

(c) VS-B1

Fig. 8. Close ups of test beams: (a) horizontal splitting crack in VS-OA3; (b) diagonal tension crack in VS-A1; and (c) crushing around loading plate in VS-B1

Toronto and incorporating the behavior models and constitutive relations of the disturbed stress field model (DSFM) (Vecchio 2000; Vecchio 2001). The DSFM is a refinement of the modified compression field theory (MCFT) (Vecchio and Collins 1986), and hence, is a smeared rotating crack model. Principal to the formulation is the consideration of compression softening effects in the concrete, due to transverse cracking, and of tension stiffening effects due to bond mechanisms between the concrete and the reinforcement. The DSFM, unlike the MCFT, also considers divergence of principal stress and principal strain directions, and takes into account slip deformations on crack surfaces.

The typical finite element meshes used to represent the Toronto beams are shown in Fig. 9; similar meshes were used for the Bresler–Scordelis beams. Meshes of 15×46, 15×56, and 15×66 eight-degree-of-freedom rectangular elements were used for the 4.1, 5.0, and 6.8 m beams, respectively. All longitudinal reinforcements were modeled using truss bar elements; all stirrup steel were modeled as smeared reinforcement. The steel loading plate, support plates, and rebar anchor plates were specifically included in the representation. To represent out-of-plane confinement effects in the concrete under the center loading plate, out-of-plane reinforcement was added to the neighboring elements; $\rho_z = 5\%$ was used for the two elements directly beneath the plate, and $\rho_z = 2.5\%$ was added to the ten elements adjacent to those two (see Fig. 9). (The out-of-plane reinforcement, considered in the analysis program, results in some strength enhancement but, more importantly, considerable ductility enhancement.) The concrete and reinforcement material properties used were as previously reported in the details of the test specimens, except for the tensile strength of concrete, which was estimated from the compressive strength as $0.33\sqrt{f_c'}$ (MPa). All constitutive modeling was done according to the default models of the DSFM. Loading was applied in a displacement-control mode (i.e., imposed midspan deflection) with a typical step size of 0.25 mm for the 4.1 and 5.0 m beams, and 0.50 mm for the 6.8 m beams.

J. Struct. Eng. 2004.130:460-469.

Table 7. Comparison of Calculated Versus Experimental Results

Beam number	Ultimate load			Midspan deflection		
	$P_{u\text{-Test}}$ (kN)	$P_{u\text{-Calc}}$ (kN)	$P_{u\text{-Test}}/P_{u\text{-Calc}}$	$\delta_{u\text{-Test}}$ (mm)	$\delta_{u\text{-Calc}}$ (mm)	$\delta_{u\text{-Test}}/\delta_{u\text{-Calc}}$
BS-OA1	334	316	1.06	6.6	12.0	0.55
BS-OA2	356	270	1.32	11.7	18.5	0.63
BS-OA3	378	294	1.29	27.9	20.8	1.34
BS-A1	468	472	0.99	14.2	15.8	0.90
BS-A2	490	399	1.23	22.9	19.5	1.17
BS-A3	468	366	1.28	35.8	44.6	0.80
BS-B1	446	423	1.06	13.7	15.3	0.90
BS-B2	400	327	1.22	20.8	19.5	1.07
BS-B3	356	355	1.00	35.3	39.0	0.91
BS-C1	312	307	1.02	17.8	18.3	0.97
BS-C2	324	258	1.26	20.1	17.3	1.16
BS-C3	270	255	1.06	36.8	36.3	1.01
		Mean	1.15		Mean	0.95
		COV (%)	11.04		COV (%)	23.65
VS-OA1	331	311	1.06	9.1	9.5	0.96
VS-OA2	320	287	1.11	13.2	12.8	1.03
VS-OA3	385	333	1.16	32.4	25.5	1.27
VS-A1	459	476	0.96	18.8	14.3	1.31
VS-A2	439	457	0.96	29.1	21.8	1.33
VS-A3	420	447	0.94	51.0	51.3	0.99
VS-B1	434	423	1.03	22.0	15.8	1.39
VS-B2	365	384	0.95	31.6	22.3	1.42
VS-B3	342	376	0.91	59.6	51.2	1.16
VS-C1	282	289	0.98	21.0	15.3	1.37
VS-C2	290	306	0.95	25.7	20.6	1.25
VS-C3	265	283	0.94	44.3	43.2	1.03
		Mean	1.00		Mean	1.21
		COV(%)	7.78		COV(%)	13.93
Total		Mean	1.07		Mean	1.08
		COV (%)	12.03		COV (%)	21.76

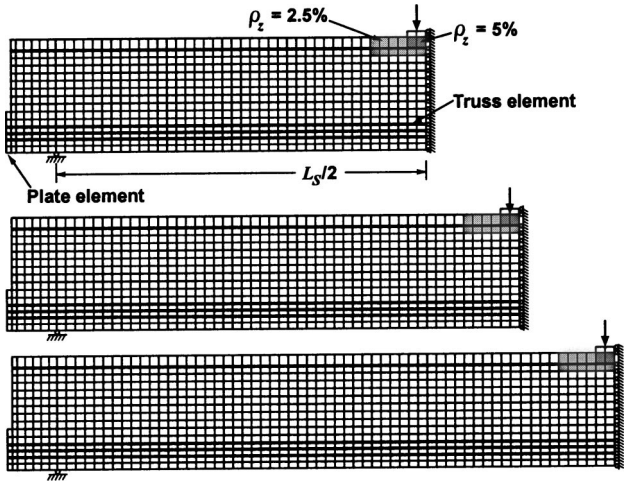

Fig. 9. Typical finite element meshes

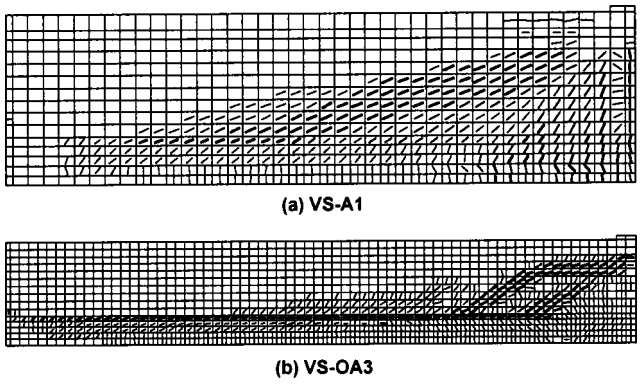

Fig. 10. Calculated cracking patterns: (a) beam VS-A1 and (b) beam VS-OA3

J. Struct. Eng. 2004.130:460-469.

The ultimate strengths calculated from the finite element analyses are compared to experimental results in Table 7 for both the Bresler–Scordelis and the Toronto set of beams. Shown in Fig. 6 are the calculated load–deflection responses for the Toronto beams. It is seen that reasonably accurate simulations of strength and load–deformation response were obtained. For the combined set of 24 beams, the ratio of the experiment-to-calculated strength ($P_{u,\exp}/P_{u,\text{calc}}$) had a mean of 1.07 and a coefficient of variation of 12.0%. Interestingly, the strengths of the Bresler–Scordelis beams were typically underestimated, while those of the Toronto beams were overestimated. The calculated load–deflection responses for the Toronto beams were slightly overestimated in terms of stiffness, falling closer to the observed responses of the Bresler–Scordelis beams. Displacements at ultimate load were generally underestimated (see Table 7). In all cases, the correct modes of failure were calculated. Crack patterns were also in reasonably good agreement with test observations (e.g., see Fig. 10).

Discussion

Despite some minor differences in material properties, construction details, and loading arrangements in the duplicate program, the Bresler–Scordelis test results were reproducible with reasonably good accuracy. This provides additional evidence of the high quality of the original test series, and supports their use as benchmark data.

Test observations indicate that nine of the 12 test beams, those containing web reinforcement, were highly influenced by concrete compression effects; that is, by crushing of concrete under the loading plate and by crushing/splitting of concrete in the flexural compression zone. While the beams were intentionally overreinforced in flexure to promote shear failures, true shear failures were observed only in the three beams containing no web reinforcement. In the short- and intermediate-length beams containing web steel, shear mechanisms had varying degrees of influence on behavior but failure was ultimately dictated by crushing, splitting, and spalling of concrete in the flexural compression zone. Shear mechanisms played little role in the behavior of the long-span beams.

In the three beams containing no shear reinforcement, final failure involved propagation of the critical diagonal tension crack into a horizontal splitting crack along the top of the uppermost layer of bottom longitudinal reinforcement. This splitting crack extended to the ends of the beams, where it diverted upwards to bypass the rebar anchor plate. As such, the anchor plates influ enced behavior, not only by averting a bond failure but also by affecting the critical crack formation.

Accurate finite element modeling of the original and replica beams is difficult, particularly if being represented by a two-dimensional membrane analysis. Influences relating to out-of-plane confinement effects and concrete tensile strength play a major role.

In the beams containing web reinforcement, the out-of-plane confinement introduced by the loading plate had a significant influence on actual and calculated response. Recognizing that crushing of concrete beneath and around the loading plate was a critical factor, it was important to account for the strength and ductility enhancement in the concrete due to the restraining effects of the loading plate. In the finite element analyses described previously, this restraint effect was approximately simulated by introducing some out-of-plane reinforcement in the adjoining concrete elements. If no out-of-plane reinforcement was used, the mean of the ratio of experiment-to-calculated strength capacities ($P_{u,\exp}/P_{u,\text{calc}}$) of the 18 beams containing web reinforcement increased from 1.04 to 1.12, with several of the analyses terminating prematurely due to crushing under the loading plate. The mean of the ratio of experiment-to-calculated deflection at ultimate ($\delta_{u,\exp}/\delta_{u,\text{calc}}$), for the 18 beams, increased from 1.12 to 1.24, indicating that a significant underestimation of ductility results if out-of-plane confinement from the plate is not considered.

For the beams containing no shear reinforcement, the concrete tensile strength played a major role in defining the failure load, with a critical diagonal tension crack forming in the web followed by tension splitting along the top of the longitudinal bars. In the finite element analyses, the concrete tensile strength was estimated from the compressive strength by the commonly used expression $0.33\sqrt{f'_c}$ (MPa). Recall that this relationship, developed by Bresler and Scordelis and subsequently included in various design codes, was chosen to intentionally give a lower bound estimate of the concrete cracking strength. The concrete split cylinder strength (f_{sp}) or modulus of rupture (f_r), on the other hand, are known to provide higher-bound estimates of the concrete tensile strength. When the finite element analyses were repeated for the six beams containing no shear reinforcement, using the measured f_{sp} values for concrete tensile strength in the Toronto beams and the measured f_r values for the Bresler–Scordelis beams, the mean of the ratio of experiment-to-calculated strength capacities ($P_{u,\exp}/P_{u,\text{calc}}$) decreased from 1.15 to 0.90, indicating a high sensitivity. The mean of the ratio of experiment-to-calculated deflection at ultimate ($\delta_{u,\exp}/\delta_{u,\text{calc}}$), for the six beams, similarly decreased from 0.96 to 0.91.

It is generally recognized that the ratio of tensile strength to compressive strength of concrete is substantially higher in young (moist) concrete, before microcracking from drying and shrinkage can have much influence. Recall that the Bresler–Scordelis beams were typically wet cured for seven days and tested on the thirteenth day, whereas the Toronto beams were tested as late as four months after casting. As such, the tensile strength of the concrete in the Bresler–Scordelis beams was likely substantially higher than in the Toronto beams, despite the concrete compressive strengths being nominally similar. As discussed, in shear-critical beams, particularly those continuing little or no shear reinforcement, behavior is heavily dependent on the concrete tension strength. Herein, likely, lies the explanation for the higher load capacities seen in the Bresler–Scordelis beams, particularly for the OA series of specimens.

Conclusions

From the experimental and analytical investigations undertaken, the following conclusions can be drawn.

1. The test results of the classic series of beams tested by Bresler and Scordelis were largely reproducible.
2. In the test beams containing no web reinforcement, sudden and brittle failures were brought on by the formation of a critical diagonal tension crack extending into longitudinal splitting crack through to the end of the beam. The bar anchor plate affected, to a minor extent, the formation of the splitting crack. These beams were genuinely shear critical.
3. In the test beams containing web reinforcement, somewhat more ductile failures developed with the crushing, splitting, and spalling of concrete in the flexural compression zone and most notably beneath and adjacent to the central loading

J. Struct. Eng. 2004.130:460-469.

plate. Although shear mechanisms played a minor role in the short- and intermediate-length specimens, these beams did not fail in a pure shear-critical manner.

4. In a finite element simulation of these test beams, three-dimensional stress effects were significant. In particular, allowing for out-of-plane confinement effects from the central loading plate was important in averting premature failure in the calculations due to crushing of concrete in the load application zone.
5. In the finite element analyses, the value used for the concrete tensile strength had significant influence on the calculated strength and response of the beams containing no web reinforcement. This value must be chosen carefully. In using the lower-bound estimate of $0.33\sqrt{f'_c}$ (MPa), one should expect underestimated beam capacities.
6. The relatively high beam shear strengths observed in the Bresler–Scordelis test beams were partly the result of the higher tension-to-compression strength ratios common in young, moist concrete.
7. The Bresler–Scordelis beams, and the duplicate series described herein, represent a valid and difficult challenge for calibrating nonlinear finite element formulations; not so much for modeling shear-critical behavior, as generally thought, but for other equally complex and important mechanisms.

Notation

The following symbols are used in this paper:

A_s = cross-sectional area of rebar or of total longitudinal tension reinforcement;
A'_s = cross-sectional area of longitudinal compression reinforcement;
b = width of beam cross section;
d = depth to center of gravity of longitudinal tension reinforcement;
d' = depth to center of gravity of longitudinal compression reinforcement;
E_c = modulus of elasticity of concrete;
f'_c = concrete compressive strength (28 day cylinder strength);
f_{sp} = concrete split cylinder strength;
f'_t = concrete tensile strength;
f_u = steel ultimate strength;
f_y = steel yield stress;
h = depth of beam cross section;
L = total length of beam;
L_s = span length of beam;
P_u = ultimate load capacity of beam;
w_f = width of concrete flexural crack;
w_s = width of concrete shear (diagonal) crack;
δ_u = midspan deflection at peak load;
ε_o = concrete strain at peak cylinder stress;
ε_s = average strain in reinforcing bar;
ρ_v = transverse (shear) reinforcement ratio; and
ρ_z = out-of-plane reinforcement ratio.

References

ASCE. (1982). "Finite element analysis of reinforced concrete." *State-of-the-Art Rep. No. ISBN 0-87262-307-6*, 545 pp.

Bresler, B., and Scordelis, A. C. (1963). "Shear strength of reinforced concrete beams." *J. Am. Concr. Inst.*, 60(1), 51–72.

Vecchio, F. J. (2000). "Disturbed stress field model for reinforced concrete: Formulation." *J. Struct. Eng.*, 126(9), 1070–1077.

Vecchio, F. J. (2001). "Disturbed stress field model for reinforced concrete: Implementation." *J. Struct. Eng.*, 127(1), 12–20.

Vecchio, F. J., and Collins, M. P. (1986). "The modified compression field theory for reinforced concrete elements subjected to shear." *J. Am. Concr. Inst.*, 83(2), 219–231.

Willam, K., and Tanabe, T. (2001). "Finite element analysis of reinforced concrete structures." *ACI Special Publ. No. SP-205*, 399 pp.

J. Struct. Eng. 2004.130:460-469.